Developmental Biology

Vascular mural cells protect the adult brain from haemorrhage but do not control the blood-brain barrier in developing zebrafish

Reviewed Preprint
v1 • February 19, 2025
Not revised

Oguzhan F Baltaci, Andrea Usseglio Gaudi, Stefanie Dudczig, Weili Wang, Maria Cristina Rondon-Galeano, Ye-Wheen Lim, James Rae, Anne Lagendijk, Robert G Parton, Alison Farley, Benjamin M Hogan

Organogenesis and Cancer Program, Peter MacCallum Cancer Centre, Melbourne, Australia • Sir Peter MacCallum Department of Oncology, University of Melbourne, Melbourne, Australia • Institute for Molecular Bioscience, The University of Queensland, Brisbane, Australia • Centre for Microscopy and Microanalysis, The University of Queensland, Brisbane, Australia • Walter and Eliza Hall Institute of Medical Research, Melbourne, Australia • Department of Anatomy and Physiology, University of Melbourne, Melbourne, Australia

eLife Assessment

This **important** study examines the role of pericytes in patterning the zebrafish blood-brain barrier (BBB) and controlling its permeability. Using pdgfrb mutant zebrafish models lacking brain pericytes, the authors report that pericyte-deficient cerebrovasculatures are ill-patterned, yet display unaltered restrictive BBB permeability properties at larval and juvenile stages. More severe phenotypes are detected in adults, with focal leakage sites associated with hemorrhages and aneurysms. Using **solid** and beautifully documented imaging, the authors suggest that, contrary to the situation described in rodent models, pdgfrb-dependent pericytes are not required to maintain the BBB in the zebrafish brain; these unexpected and intriguing findings reshape our understanding of BBB permeability regulation in vertebrates.

https://doi.org/10.7554/eLife.104061.1.sa3

Abstract

The blood-brain barrier (BBB) protects the brain from circulating metabolites and plays central roles in neurological diseases. Endothelial cells (ECs) of the BBB are enwrapped by mural cells including pericytes and vascular smooth muscle cells (vSMCs) that regulate angiogenesis, vessel stability and barrier function. To explore mural cell control of the BBB, we investigated neurovascular phenotypes in zebrafish *pdgfrb* mutants that lack brain pericytes and vSMCs. As expected, mutants showed an altered cerebrovascular network with mis-patterned capillaries. Unexpectedly, mutants displayed no BBB leakage from larval through to young adult stages. This demonstrates that pericytes and vSMCs do not control BBB function in young zebrafish. Instead, we observed adult BBB disruption occurring at "hotspot" focal haemorrhages at major vessel aneurysms. ECs at leakage hotspots showed

induction of caveolae on abluminal surfaces and major structural defects including basement membrane thickening and disruption. Our work suggests that capillary pericytes regulate cerebrovascular patterning in development and vSMCs of major arteries protect from haemorrhage and BBB breakdown in older zebrafish. The fact that young zebrafish can have a conserved BBB with intact barrier function in the absence of mural cells, warrants renewed interrogation of the paradigm of mural cell control of the BBB.

Main text

Neurovascular endothelial cells (ECs) have unique functional and structural properties to regulate substance exchange between blood and brain, establishing the blood-brain barrier (BBB)[1,2]. Loss of normal BBB function is associated with neuropathological states, including neurodegeneration, infection and cancer[1,2]. Mural cells are vascular support cells that include pericytes and vascular smooth muscle cells (vSMCs) and control vascular development, function and BBB permeability[3–9]. PDGFB/PDGFRβ signalling is required for the development of mural cells[3,4,10–12] and their depletion in PdgfB or Pdgfrβ deficient rodents causes altered angiogenesis, aneurysm and vessel leakiness[3–6,13]. Strikingly, rodent models of pericyte loss have an open BBB, with free transport of tracer dyes from the blood stream into the brain parenchyma but an otherwise intact vasculature[5,6]. These and other observations, have led to a current model whereby pericytes control BBB function by suppressing EC adsorptive transcytosis. This prominent mechanism holds significant translational promise to safely open up the BBB in therapeutic settings, by discovering ways to disrupt pericyte control of ECs[5,14].

Zebrafish have a highly conserved BBB[15–19] with the brain endothelium expressing conserved molecular markers of a functional BBB[18] and showing conserved cellular interactions with pericytes, smooth muscle cells and glial cells[20,21]. The zebrafish BBB becomes functional by 5 days post fertilisation (dpf)[19] and as in mice, *pdgfrb* mutants lack brain pericytes and exhibit loss of vSMCs[13,20]. Thus, the zebrafish is accepted as a highly accessible model to study BBB function and mural cell control of the BBB[17]. To investigate the influence of mural cells upon the neurovasculature, we generated a *pdgfrb* mutant (*pdgfrb*^{uq30bh}), which possesses an early deletion leading to a frameshift, predicted to cause a premature stop codon and a putative null allele. Using the *TgBAC(pdgfrb:egfp)*^{ncv22} line, we observed that pericytes were lost in the cerebral central arteries of *pdgfrb* mutants (**Fig. 1a**), as in previous studies[13,20]. To assess how brain angiogenesis occurs without pericytes, we imaged, traced and quantified blood vessel branching from the middle mesencephalic central arteries in the midbrain (**Fig. 1a-c**; **Extended Data Fig. 1a**). At 7 dpf, mutants displayed significantly reduced vascular complexity compared to siblings, with reduced vessel length and branch points (**Fig. 1d-e**). This was more severe at 14 dpf, demonstrating the phenotype is progressive (**Fig. 1d-e**). Timecourse imaging revealed the reduction in vascular complexity was apparent from 5 dpf (**Extended Data Fig. 1a-b**). These results suggest that pericytes (the vSMCs only begin to develop after 5 dpf[22]) regulate angiogenesis from early in larval development.

We next tested BBB function in mutants at 7 and 14 dpf. We performed intravenous injection of fluorescently conjugated tracers of various molecular weights (1 kDa NHS, 10 kDa and 70 kDa Dextran), and live imaged fish at 2 hours after injection (as in [19]) (**Fig. 1f**; **Extended Data Fig, 1c**). 2000 kDa Dextran was coinjected to normalize quantification of vascular tracer dye delivery (see methods for details). We found no evidence of 10 kDa or 70 kDa Dextran tracer extravasation into the brain parenchyma of *pdgfrb*^{uq30bh}mutants at either timepoint (**Fig. 1g**; **Extended Data Fig. 1c-e**). 1 kDa tracer showed no difference between genotypes but was observable in the parenchyma in both sibling and mutants, indicating the smaller cargo can pass the BBB (**Extended Data Fig. 1c & e**). Together, these results show that neither pericytes nor vSMCs play a role in establishment of BBB function in larval zebrafish.

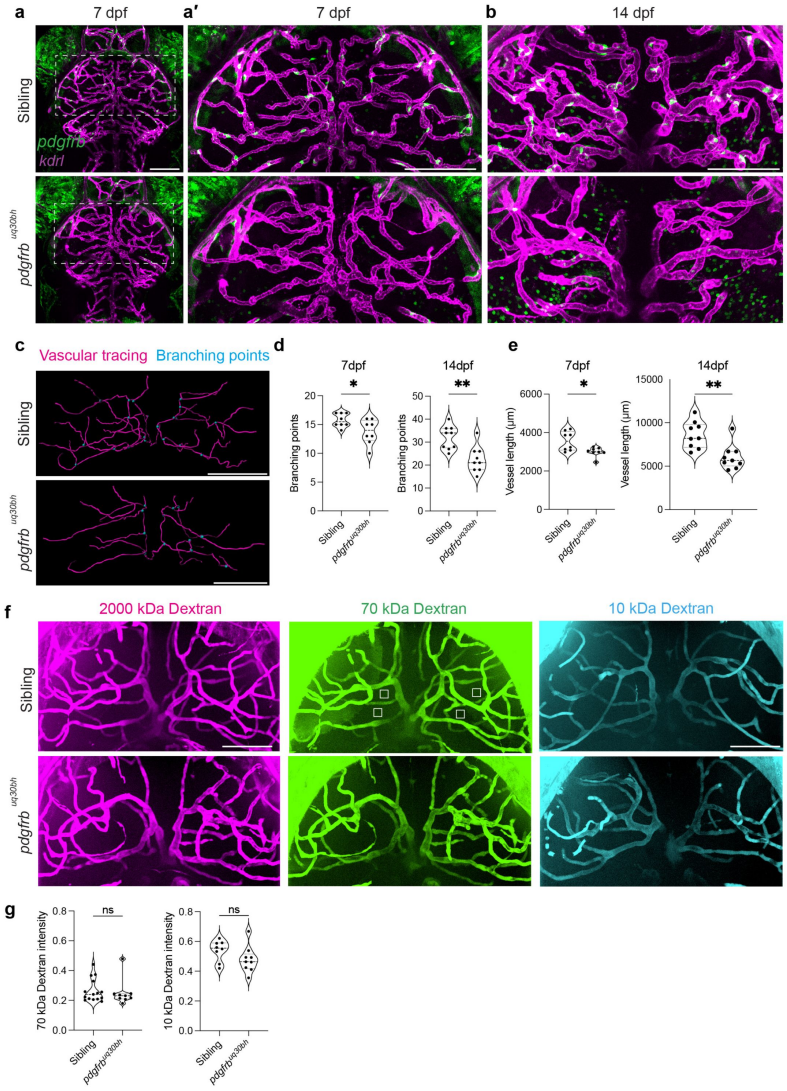

Fig. 1

Pericyte-deficient larval brain vasculature displays abnormal patterning but an intact blood-brain barrier

a, Confocal projections of pericytes (*TgBAC(pdgfrb:egfp)*^{ncv22}) and brain vasculature (*Tg(kdrl:Hsa.HRAS-mCherry)*^{s843}) in sibling and *pdgfrb*^{uq30bh} mutants at 7 dpf.
a', Zoomed section from **a** (dashed rectangle) showing the midbrain central arteries.
b, Midbrain central arteries in sibling and *pdgfrb*^{uq30bh} mutants at 14 dpf.
c, Representative images of vascular tracing at 7 dpf using Imaris 10.1 software. Lumenized blood vessels branching from the middle mesencephalic central arteries in the midbrain were traced.
d,e, Quantification of midbrain vessel length (**d**) and branching points (**e**). N=8 per group, unpaired *t*-test, **P*<0.05, ***P*<0.01.
f, Fluorescent tracer assays in the midbrain of zebrafish larvae. 10 kDa Dextran–Cascade Blue and 70 kDa Dextran–Fluorescein were used to detect tracer extravasation to the brain parenchyma (white squares) in separate experiments and were coinjected with 2000 kDa Dextran–Tetramethylrhodamine to normalize vascular tracer intensity. Representative image of 2000 kDa Dextran was taken from 70 kDa Dextran coinjection, and 10 kDa Dextran coinjection is shown in **Extended Data Fig. 1**.
g, Quantification of brain parenchymal 70 kDa and 10 kDa Dextran intensity normalized to the vascular 2000 kDa Dextran intensity. N=15 in sibling and n=7 in *pdgfrb*^{uq30bh} for 70 kDa Dextran intensity, n=8 in sibling, n=9 in *pdgfrb*^{uq30bh} for 10 kDa Dextran intensity. Unpaired *t*-test, ns=not significant.
a,a', b, c, f, Scale bars: 100 µm.

To investigate how mural cells control cerebral vasculature at later stages of life, we tissue-cleared brains of adult stage *pdgfrb*^{uq30bh}mutants and siblings[23] and performed whole brain imaging. We confirmed loss of pericytes and vSMCs at this stage (**Fig. 2a**). We examined a consistent region of the left optic tectum (mid brain) and detected decreased branching of capillaries and increased diameter of major vessels (**Fig. 1b-d**). This vessel dilation was restricted to larger calibre arteries that would normally be invested with vSMCs and not seen in capillaries (**Fig. 1c-d**). This suggests vessel dilation in mutants is due to loss of vSMCs and reduced branching of capillaries to loss of pericytes.

We assessed BBB function in juvenile 2-month-old zebrafish by intravenous tracer injection (as in [24]) and using a mixture of 70- and 2000 kDa Dextran. We euthanized fish 2 hours post-injection and tissue-cleared the brains. The whole brain imaging revealed that mutants displayed widespread aneurysm of major vessels (**Fig. 2e-f**, **Extended Data Fig. 2a-a'**). To quantify potential BBB leakage, we imaged a consistent region with high capillary density (**Fig. 2e'**), and quantified parenchymal 70 kDa Dextran intensity relative to vascular 2000 kDa Dextran intensity. Both tracers remained restricted to the vascular lumen regardless of the severity of the aneurysms (**Fig. 2g**). This correlates with our findings at larval stages and demonstrated that mural cells are dispensable for the establishment and early maturation of the BBB in zebrafish up to 2 months of age.

To investigate BBB integrity at later stages, we injected 3-month-old adult zebrafish with 10 or 70 kDa Dextran. Brightfield imaging of vibratome sectioned brains revealed severe aneurysms across large calibre vessels (**Fig. 3a**) with blood pooling that was potentially consistent with vessel ruptures (**Fig. 3c**). Furthermore, we detected parenchymal accumulation of tracer dye closely associated with large calibre vessel aneurysms (**Fig. 3b-c**; **Extended Data Fig. 3a-á**). To quantify the distribution of parenchymal tracer dye from deep (around major artery aneurysms) to superficial (in capillary beds) brain regions, we measured fluorescence intensity in 10 brain regions 100 microns apart from medial to lateral locations. This demonstrated accumulation of tracer dye in medial regions associated with aneurysm in mutants, with no evidence of major leakage in capillary beds (**Fig. 3d-e**). To better understand the extravasated tracer accumulation, we conducted whole brain imaging after 70 kDa Dextran injection. Interestingly, we observed highly localised tracer accumulated in regions that could be considered leakage "hotspots" at large calibre vessel aneurysms (**Fig. 4a**; **Extended Data Fig. 4a**; Supplementary Videos 1 and 2). Quantification of three independent whole cleared brains throughout the optic tecta revealed on average 11 hotspots occurring at major vessels in each mutant animal (**Fig. 4b**). To further understand the nature of these hotspots, we examined red blood cells in *pdgfrb* mutant adults (Crispants, validated in **Extended Data Fig. 4b**) using the *Tg(gata1:DsRed)*^{sd2} transgenic line together with tracer injection. These animals showed that tracer accumulation occurred concomitant with extravasated red blood cells at hotspots, identifying them as focal haemorrhages (**Fig. 4c**). Notably, these sites were not detected at capillaries (**Fig. 4d**). Taken together, this shows that in older mutants, loss of BBB integrity is associated with focal haemorrhage along aneurysmal vessels.

Pericytes are proposed to regulate the BBB by suppressing adsorptive transcytosis through brain capillary ECs[5,6]. This model is built on the observation by electron microscopy of the induction of caveolae in leaky pericyte deficient vessels[5,6]. To investigate if the loss of BBB integrity is associated with ultrastructural changes, we performed electron microscopy. We imaged large calibre vessels and capillaries (**Fig. 4e**; **Extended Data Fig. 4c**) and examined cellular junctions, basement membrane and caveolae (defined as uncoated vesicular profiles of <100nm diameter). While tight junctions between endothelial cells remained intact (**Fig. 4f**), Caveola density along the large vessel aneurysms in *pdgfrb*^{uq30bh} mutants was significantly increased. This increase was almost exclusive to the abluminal side of the ECs (**Fig. 4g**). This abluminal accumulation of caveolae may be more associated with changes in the mechanical state of ECs (as caveolae are highly regulated by membrane tension[25,26]) than changes in

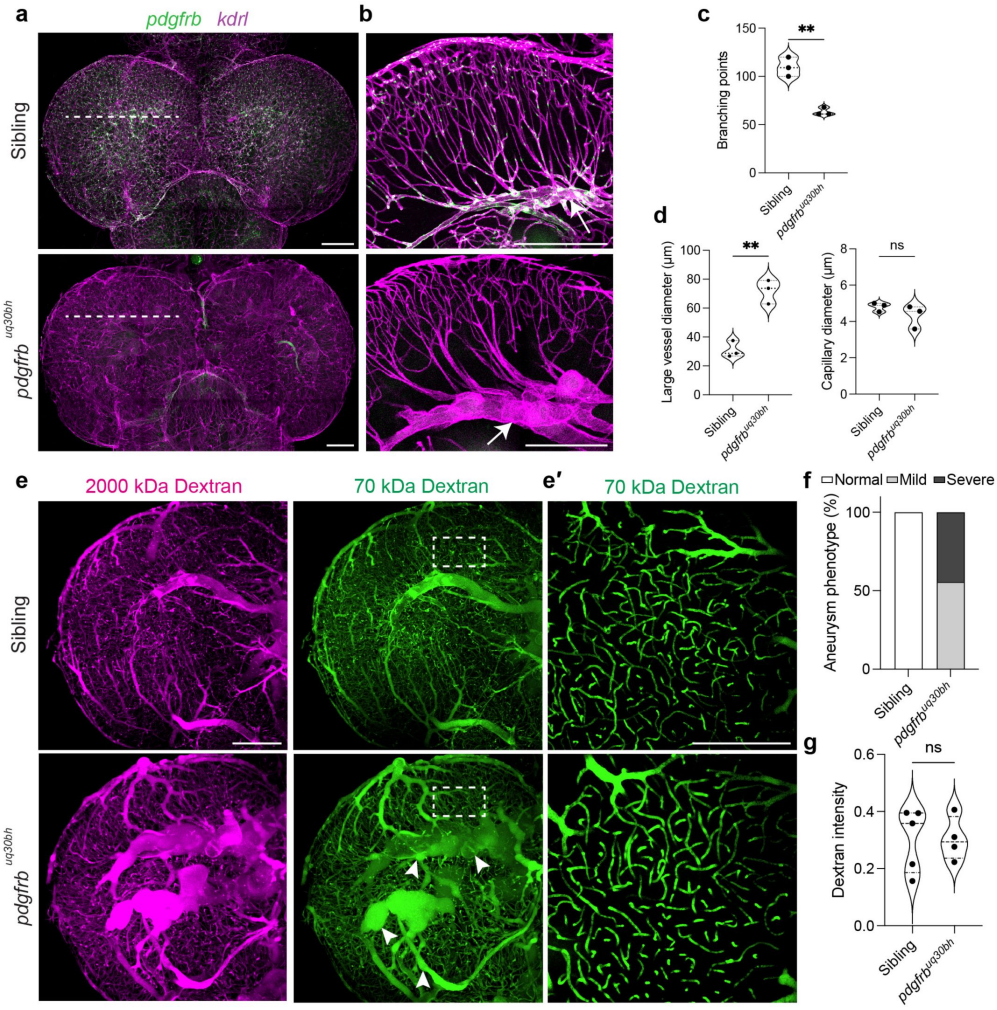

Fig. 2

pdgfrb^{uq30bh} mutants develop aneurysms but display an intact blood-brain barrier at 2 months of age.

a, Confocal projections of whole brain imaging showing mural cells (*TgBAC(pdgfrb:egfp)*^{ncv22}) and brain vasculature (*Tg(kdrl:Hsa.HRAS-mCherry)*^{s843}) in sibling and *pdgfrb*^{uq30bh} mutants at 5-months of age.
b, Restricted regions from the whole brain imaging in **a** (approximate location of dotted line) indicating pericyte loss and abnormal capillary network patterning. 100-µm thick maximum intensity projections (MIP) were generated using the continuation of the left middle mesencephalic central artery (arrow) as an anatomical anchor point.
c, d, Quantification of capillary branching points, large vessel and capillary diameter using the area shown in **b**. Large vessel diameter was quantified by averaging 5 points per vessel and the capillary diameter was quantified by averaging 10 capillary diameter per sample. N=3 per group, unpaired *t*-test, ***P*<0.01, ns=not significant.
e, Fluorescent tracer assays in the midbrain of 2-month-old zebrafish. 70 kDa Dextran– Fluorescein and 2000 kDa Dextran–Tetramethylrhodamine were co-injected to detect the tracer extravasation to the brain parenchyma and the tracer within the vasculature, respectively. Arrowheads indicate examples of aneurysms.
e', Confocal projections zoomed in on the approximate area shown in **e** (dashed rectangle). 30-µm thick MIPs were generated to examine the capillary leakage, starting 30 µm below the most superficial point of the left hemisphere of the brain to prevent the potential leakage from the superficial vessels.
f, Quantification of the severity of aneurysms in sibling (n=11) or *pdgfrb*^{uq30bh}(n=11). For examples of "severe" and "mild" see **Extended Data Fig. 2**.
g, Quantification of the brain parenchymal 70 kDa Dextran intensity normalized to the vascular 2000 kDa Dextran intensity, n=5 in sibling, n=4 in *pdgfrb*^{uq30bh} mutants, unpaired *t*-test, ns=not significant.
a, b, e, e', Scale bars: 250 µm.

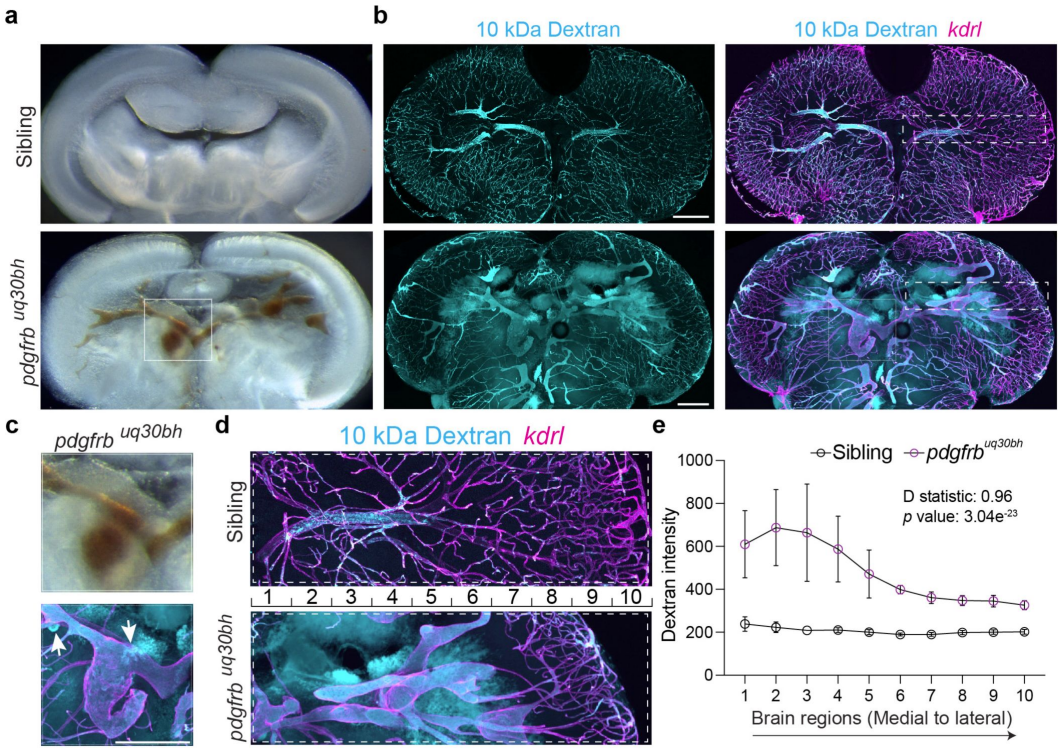

Fig. 3

Adult *pdgfrb*^{uq30bh} mutants display aneurysms and vascular integrity defects.

a, Representative images of coronal midbrain sections obtained from 3 month-old sibling and *pdgfrb*^{uq30bh} animals.
b, Fluorescent tracer assays in 3-month-old sibling and *pdgfrb*^{uq30bh}mutant animals. 10 kDa Dextran–Cascade Blue (cyan) was retro-orbitally injected, and *Tg(kdrl:Hsa.HRAS-mCherry)*^{s843} was used to label the blood vessels (magenta). Scale bar: 250 µm.
c, Zoomed regions from **a** and **b** (dotted squares) displaying blood and tracer accumulation (arrows).
d, Zoomed regions from **b** (dashed rectangle) displaying vasculature and tracer dye leakage from medial (large vessel) to lateral (capillary region) locations. The area was divided into 10 regions every 100 µm for tracer leakage quantification.
e, Quantification of brain parenchymal dextran intensity at medial (large vessel) to lateral (capillary region) locations shown in **d**. N=5 in sibling, n=4 in *pdgfrb*^{uq30bh}, Two-sample Kolmogorov-Smirnov test, error bars represent SEM.

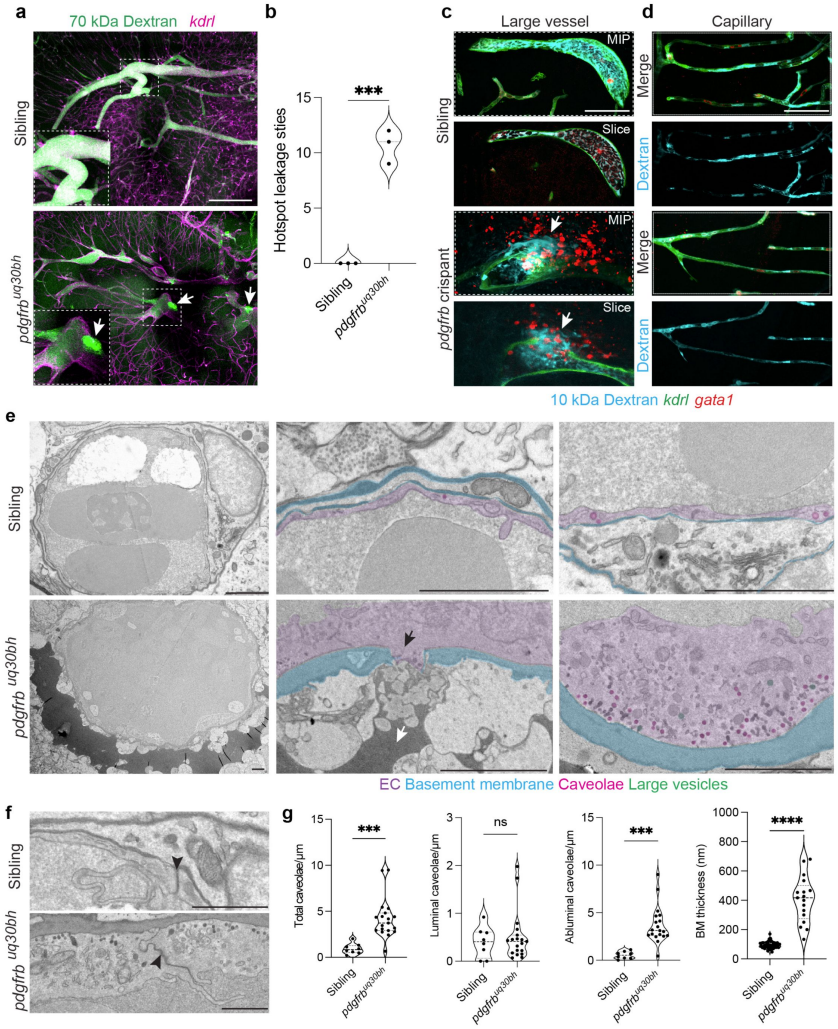

Fig. 4

Adult *pdgfrb* mutants display structural endothelial cell defects, vessel rupture and tracer accumulation at aneurysm hotspots.

a, Sections from whole brain imaging showing brain vasculature (*Tg(kdrl:Hsa.HRAS-mCherry)*^{s843}) and 70 kDa Dextran Fluorescein at 5-months of age. Inset images within dashed rectangle show areas of hot spot leakage sites (arrows).
b, Quantification of hotspot leakage sites per animal in the midbrain region. N=3 for each group, unpaired *t*-test, ***P<0.01.
c, d, High resolution imaging of large calibre vessels and capillary zones in brain regions of *pdgfrb* crispants and uninjected siblings at 10-week-old stage. 10 kDa Dextran–Cascade Blue (cyan) injected, blood vessels (*Tg(kdrl:EGFP)*^{s843}) and red blood cells (*Tg(gata1:DsRed)*^{sd2}) are shown in MIPs and single Z-sections **(c).** Hotspot leakage sites are indicated by arrows. Capillary zones are shown in MIPs for all three channels and the single 10 kDa Dextran channel showing a lack of hotspot leakage site **(d)**.
e, Transmission electron microscopy images of sectioned adult zebrafish brain vessels. *pdgfrb*^{uq30bh} mutants showed basement membrane thickening and breakdown (cyan, black arrow), serum accumulation outside the vessels (white arrow), increased abluminal endothelial caveolae (magenta). Pseudo colours shown are ECs (purple), basement membrane (cyan), caveolae (magenta) and vesicles larger than 100 nm (green). Scale bars: 2 µm.
f, Zoomed regions from **(e)** showing intact tight junctions (arrowheads) in both siblings and *pdgfrb*^{uq30bh} mutants. Scale bar: 1 µm.
g, Quantification of endothelial caveolae and basement membrane thickness. Caveolae were defined as uncoated spherical profiles <100 nm in diameter and scored as luminal or abluminal (see methods). Measurements were made for n=3 vessels for each group and a total of 8 different cellular regions measured for siblings and 19 for mutants. Basement membrane thickness was scored in 6 different regions per vessel with n=8 vessels in siblings and n=4 vessels in *pdgfrb*^{uq30bh} mutants. Unpaired *t*-test, ***P<0.001, ****P<0.0001, ns= not significant.

intracellular transport. Furthermore, we detected thickening of basement membrane (BM) (**Fig. 4g**), gaps in the BM and fluid accumulation outside the vessel wall at aneurysms in mutants. We found no obvious difference in the caveolae density of capillary ECs of *pdgfrb*^{uq30bh} mutants compared with siblings (**Extended Data Fig. 4d**). Thus, leakage hotspots at aneurysms are associated with a failure of the normal flattening of ECs, caveola induction and disruption of the BM, all factors that could contribute to or be observed concurrent with vessel wall rupture.

Brain vasculature is endowed with mural cells that control vascular development and stability[3,4,13,27]. Studies in rodents have shown that pericytes regulate BBB integrity[5,6]. This is currently thought to be caused by hotspots of increased EC transcytosis[14], rather than mechanisms such as altered cell-cell adhesion (eg, Cldn5[14]), control of Mfsd2a[19,28], Netrin1- Unc5B signalling[29] or vitronectin regulation of integrin receptors[30]. However, some studies in rodents have reported loss of pericytes without vessel leakage[31]. We show mural cells are involved in cerebrovascular patterning in larval, juvenile and young adult animals but these vessels maintain BBB function in the absence of mural cells. In our mutants, major arteries progressively harbour aneurysms. This aneurysm is likely associated with loss of vSMCs[13]. At later stages, adult mutants show leakage at hotspots distributed along aneurysms, which are focal haemorrhages. In some PDGFB/PDGFRβ mouse mutants, haemorrhages have been reported, but not in mild or hypomorphic mutants such as those used in BBB studies[3,4,12]. In our model, BBB leakage appears to only be observed once haemorrhage is present. Of course, these observations could represent a species-specific divergence from the mammalian BBB. However, the zebrafish BBB appears highly conserved with that of mammals[17] and we would argue that the importance of BBB function for vertebrate brain physiology throughout evolution makes divergence unlikely. We suggest that a deeper analysis of the nature of hotspot leakage in mural cell deficient mammalian models is warranted. Altogether, a deeper understanding of the fundamental biology of the BBB will pave the way for increasingly sophisticated efforts to target the BBB in disease in the future.

Acknowledgements

This project was supported in part by funding from Bright focus (A2018807S) and the Australian Research Council (ARC) (DP210102712) and The Brain Cancer Centre (founded by Carrie's Beanies for Brain Cancer). B.M.H was supported by a National Health and Medical Research Council Senior Research Fellowship (1155221). O.F.B was supported by the Brain Cancer Centre Blood-Brain Barrier Program. R.G.P was supported by an ARC Laureate Fellowship (FL210100107). We thank the Centre for Advanced Histology and Microscopy (RRID:SCR_025432) at the Peter MacCallum Cancer Centre and Microscopy Australia Research Facility at the Centre for Microscopy and Microanalysis at The University of Queensland. We also thank Kelly Smith and Marcos Sande Melon for academic discussions and technical suggestions.

Additional information

Author contributions

O.B performed, analysed experiments and co-wrote manuscript. B.M.H, _onceptualized experiments, analysed data and co-wrote manuscript. A.U.G, S.D, W.W, M.C.R.G, Y.W.L, J.R, R.P, A.L and A.F performed and analysed experiments.

Supplementary materials

Zebrafish husbandry

Zebrafish work was conducted in compliance with animal ethics committees at the Peter MacCallum Cancer Centre, The University of Melbourne and The University of Queensland. Previously published transgenic lines were *TgBAC(pdgfrb:egfp)*^{ncv22} [1],*Tg(kdrl:Hsa.HRAS-mCherry)*^{s843} [2], *Tg(kdrl:EGFP)*^{s843} [3] and *Tg(gata1:DsRed)*^{sd24}.

Genome editing and genotyping

The *pdgfrb*^{uq30bh} mutant strain was generated using CRISPR/Cas9-mediated genome editing. The resulting allele carries a 39-bp deletion and a 5-bp insertion in exon 3 of *pdgfrb* (ENSDARG00000100897), causing a frameshift and premature stop codon.

The gRNA sequence and genotyping primers used were: gRNA binding site: 5' GATGGTGACTAAGACGCGA 3' Forward genotyping primer: 5' CTTCCTTAGATCCTGACGTGTG 3' Reverse genotyping primer: 5' TATTGATGGGTTCGTCACCAG 3'

The *pdgfrb* F0 crispants used were generated as F0 Animals by CRISPR/Cas9-mediated genome editing using predesigned Alt-R CRISPR-Cas9 gRNAs (IDT). The gRNA sequence and genotyping primers used were: Dr.Cas9.PDGFRB.1.AA: 5' GATGGTGACTAAGACGCGAG 3'

Forward genotyping primer: 5' CTTCCTTAGATCCTGACGTGTG 3' Reverse genotyping primer: 5' TATTGATGGGTTCGTCACCAG 3' Dr.Cas9.PDGFRB.1.AB: 5' CTCGGTGCACACATAAACCC 3'

Forward genotyping primer: 5' GACGAGAACATCCCAGACTTTC 3' Reverse genotyping primer: 5' GCGTGTAAACAAATCCTAACGG 3'

Tracer dye injections and imaging

For all injections at larva and juvenile stages, NHS Ester–Alexa Fluor 405 (Thermo Fisher: A30000) or 10 kDa Dextran–Cascade Blue (Thermo Fisher: D1976) or 70 kDa Dextran– Fluorescein (Thermo Fisher: D1822) were mixed and co-injected with 2000 kDa Dextran– Tetramethylrhodamine (Thermo Fisher: D7139). This allowed for the normalisation of dye signal relative to the larger molecular weight 2000 kDa tracer to ensure that the amount injected intravenously was appropriately controlled for in all imaging experiments. A final concentration of 5 mg/ml for each tracer was used in all injections.

7 dpf larvae were anesthetised with tricaine and mounted laterally with 0.5% low-melting point agarose (Bio-Rad, 1613112) in E3 embryo water on a 35-mm glass bottom dish (MatTek: P35G-1.5-20-C). 5nl of the tracer mix was injected into the posterior cardinal vein (PCV) and larvae were recovered from agarose using a glass pipette into E3 embryo water. 14 dpf larvae were anesthetised with tricaine, placed laterally on a 3% agarose injection mold. 10 nl tracer mix was injected into the PCV and larvae were recovered in E3 embryo water.

For live imaging, larvae were mounted ventrally with 0.5% low-melting point agarose in E3 embryo water on a 35-mm glass bottom dish. All larvae were carefully live imaged at 2 hours post injection, with a maximum variation in timing of 15 minutes due to the sequential imaging, using Nikon TiE with Yokogawa CSU-W1 spinning disk with Andor Sona sCMOS camera, 40X 1.15 NA water immersion objective for 7 dpf larvae and 20X 0.75 NA objective for 14 dpf (1 um z-step for each stage).

Injections at juvenile and adult stages were performed retro-orbitally using a glass capillary needle as previously described[5]. For juvenile stage (2-month post fertilisation), brains were extracted 2 hours post injection and whole brains were tissue-cleared using the CUBIC-based method previously described[6]. Briefly, brains were fixed in 2% paraformaldehyde (PFA) at 4°C overnight, washed in PBS, incubated in CUBIC-L solution at 37°C overnight, washed and incubated in PBS at 4°C overnight, then incubated in CUBIC-R solution at room temperature overnight. Brains were mounted ventrally with 2% agarose in CUBIC-R on a 35-mm glass bottom dish and imaged using Nikon TiE with Yokogawa CSU-W1 spinning disk with Andor Sona sCMOS camera, 4X 0.2 NA objective, 10X 0.45 NA objective, and 20X 0.75 NA objective. For adult stage (>2.5-months post fertilisation), Cascade Blue 10- or 70 kDa Dextran were injected as previously described[5]. Brains were extracted 2 hours post injection, fixed in 2% PFA overnight, washed in PBS. For vibratome sectioning, brains were embedded in 7% low- melting agarose in PBS in cryomolds (Tissue-Tek) and were sectioned coronally using a vibrating microtome (Leica VT1000 S) with 200 µm thickness setting. Selected sections were placed on a microscope slide and were incubated with RapiClear 1.52 solution (SunJin Lab, RC152201) for 3 hours at room temperature. Imaging was performed using Olympus FV3000 confocal microscope with 10X 0.4 NA objective with 5 µm step size and 40X 1.4 NA oil immersion objective with 1 µm step size. For whole brain imaging, brains were tissue cleared as described earlier and were imaged using Olympus FV3000 confocal microscope with 10X 0.4 NA objective with 5 µm step size. Videos highlighting the “hotspot” leakage sites were generated using Imaris 10.1 software (Bitplane) and Adobe Premier Pro 2024.

Live imaging of pericytes and blood vessels was conducted using Olympus FV-MPERS multiphoton microscope with 25X 1.05 NA water dipping objective with 3 µm step size. To ensure optical transparency, live imaging was conducted in F0 knockout animals for the gene *slc45a2* (ENSDARG00000002593) as previously described[7] or 0.003% PTU was applied to the embryo water at 1 dpf.

Transmission electron microscopy

Brains were extracted from euthanised 5-month-old zebrafish, fixed in 2.5% glutaraldehyde for 1 hour at room temperature and washed with PBS. For sectioning, the brains were embedded in 7% low-melting point agarose in PBS in cryomolds (Tissue-Tek) and were sectioned coronally using a vibrating microtome (Leica VT1000 S) with 200 µm thickness. Tissue sections were processed as described previously[8].

Briefly, tissue sections were immersed consecutively in a series of aqueous solutions: 1.5% potassium ferricyanide and 2% osmium tetroxide, 1% thiocarbohydrazide, 2% osmium tetroxide, 2% uranyl acetate and 0.06% lead nitrate using a Pelco Biowave at 80W under vacuum for 3min each. Vibratome sections then underwent serial dehydration in increasing concentrations of ethanol, before serial infiltration with increasing concentrations of Procure 812 resin. Ultrathin sections were obtained using a Leica UC64 ultramicrotome and imaged on a Jeol JEM-1011 at 80kV.

Quantifications

Vessel length, diameter and branching points

Vessel length, diameter and branching points were quantified using Imaris 10.1 software (Bitplane). For larval stages, lumenized midbrain central artery (*kdrl:Hsa.HRAS-mCherry)* branching from the middle mesencephalic arteries was traced using the filament tool and the total filament length (µm) was plotted. The branching points within the traced blood vessels were quantified by manual scoring in 3D view. For adult stage, 100-µm thick maximum intensity projections (MIP) were generated from whole brain imaging, using the continuation of the left

middle mesencephalic central artery as an anatomical anchor point as the consistent region measured. For diameter measurements, 10 capillary diameters were measured per sample. Vessel anatomy was identified using the study by Isogai et al[9] as a reference.

Tracer intensity

Tracer intensity quantification was performed on genotype blinded image sets using Fiji[10]. For larval stage experiments, the tracer accumulation in brain parenchyma (70-or 10 kDa Dextran or 1 kDa NHS Ester) was calculated using average intensity from 4 midbrain parenchymal regions in 50-µm thick MIPs, which were generated starting from 50 µm below dorsal longitudinal vessel (DLV) to avoid detecting potential leakage from surface vessels. These measurements were normalized to the vascular tracer intensity of 2000 kDa Dextran, which was calculated using average intensity from 4 regions within the DLV lumen. As such, for each data point: intensity=parenchymal dextran (1, 10 or 70 kDa) intensity/luminal 2000 kDa Dextran intensity.

For juvenile stage experiments, 30-µm thick MIPs were generated starting from 60 µm below the most superficial vessel to potential leakage from the surface vessels. Brain parenchymal 70 kDa Dextran intensity was calculated using average intensity from 4 midbrain parenchymal regions and was normalized to vascular 2000 kDa Dextran intensity, which was calculated using average intensity from 4 regions within the lumen of superficial large calibre vessels. For adult stage experiments, 50-µm thick MIPs were generated and dextran intensity outside the vessels was measured at every 100 µm from medial to lateral direction within 1 mm. Branching point of left and right middle mesencephalic arteries was determined as the starting point.

TEM quantification

Imaged sections were quantified using Fiji[10]. Caveolae were defined as circular profiles of less than 100 nm in diameter and were scored as luminal or abluminal based on proximity to each surface membrane (within 500 µm of each surface or in a thin walled vessel the caveolae closest to each surface). Basement membrane thickness was scored in 6 different locations per vessel that were selected at random. N=3-8 vessels per group were analysed as indicated in the Figure legends.

Statistical analysis

Statistical analyses and graphical representations were conducted using GraphPad Prism 10 software. ns: $P>0.05$, *$P\leq0.05$, **$P\leq0.01$, ***$P\leq0.001$, ****$P\leq0.0001$. For **Figure 3e**, we applied the non-parametric two-sample Kolmogorov-Smirnov test using Python software to evaluate whether the distribution of tracer accumulation for each position differed from that of the control. Further details on statistics can be found in each figure legend.

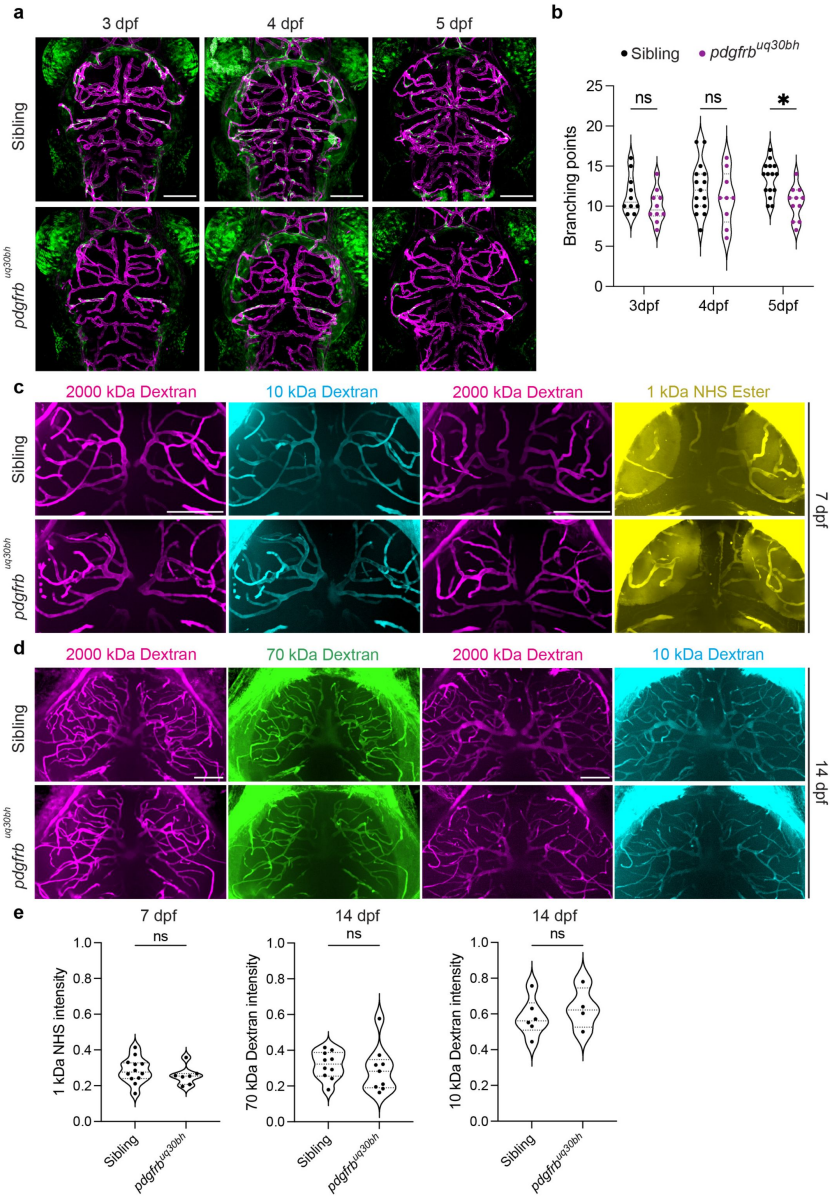

Extended Data Fig. 1

pdgfrb^{uq30bh} larvae exhibit decreased cerebrovascular complexity but an intact BBB.

a, Confocal projections of pericytes (*TgBAC(pdgfrb:egfp)*^{ncv22}) and brain vasculature (*Tg(kdrl:Hsa.HRAS-mCherry)*^{s843}) in sibling and *pdgfrb*^{uq30bh} mutants at 3-5 dpf.

b, Quantification of branching points of midbrain central arteries demonstrating the first detectable vessel patterning phenotype is seen at 5 dpf. N=10 per group at 3 dpf, n=15 in sibling and n=9 in *pdgfrb*^{uq30bh}at 4 dpf, n=15 in sibling and n=11 in *pdgfrb*^{uq30bh} at 5 dpf. Unpaired *t*-test, ns=not significant, *P<0.05.

c, d, Fluorescent tracer leakage assays in the midbrain of zebrafish larvae at 7 (**c**) and 14 dpf (**d**). 70 kDa Dextran–Fluorescein, 10 kDa Dextran–Cascade Blue and 1 kDa NHS Ester–Alexa Fluor 405 were used to detect tracer extravasation to the brain parenchyma in separate experiments and were coinjected with 2000 kDa Dextran–Tetramethylrhodamine to normalize vascular tracer intensity.

e, Quantification of brain parenchymal 70- and 10- and 1 kDa tracer intensity normalized to vascular 2000 kDa Dextran intensity. N=12 for sibling and n=7 in *pdgfrb*^{uq30bh} 1 kDa NHS Ester intensity at 7 dpf, n=10 in sibling and n=9 in *pdgfrb*^{uq30bh} for 70 kDa intensity at 14dpf, n=6 for sibling and n=4 for *pdgfrb*^{uq30bh} for 10 kDa intensity at 14 dpf. Unpaired *t*-test, ns=not significant.

a, c, d, Scale bars: 100 μm.

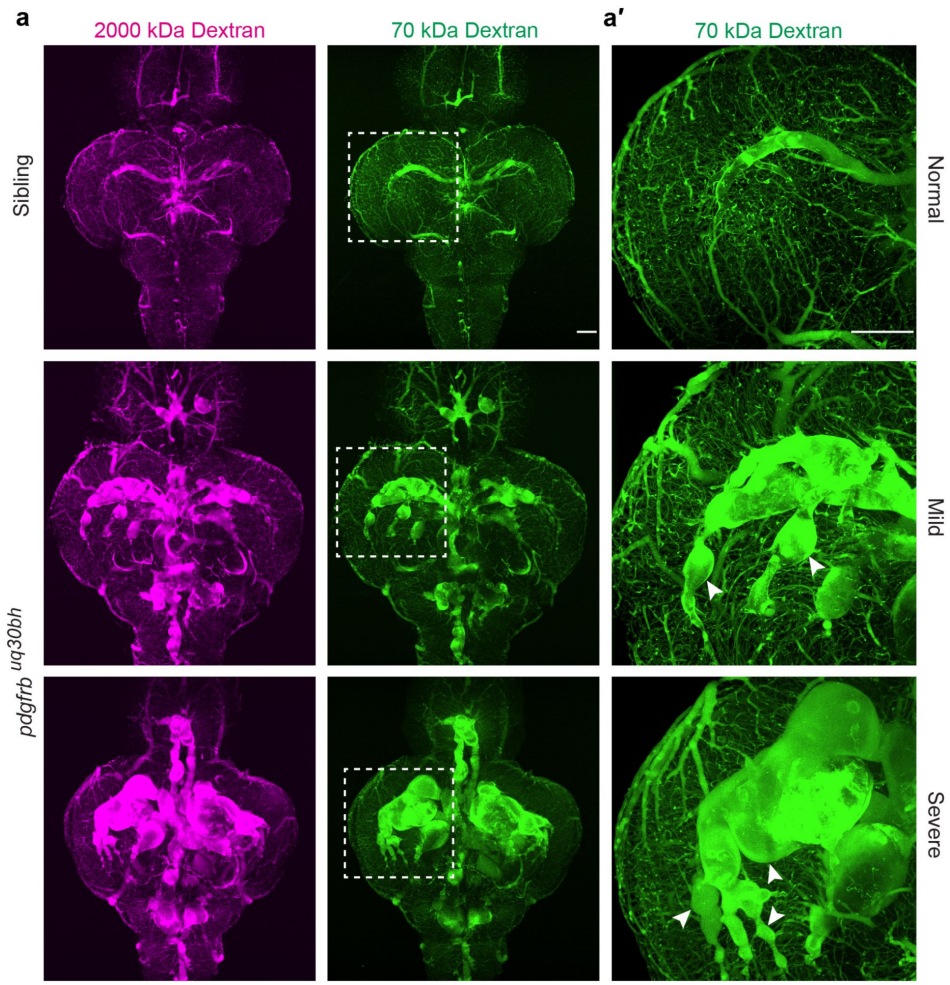

Extended Data Fig. 2

Examples of aneurysms in *pdgfrb*^{uq30bh} mutants at 2-month-old stage.

a, Fluorescent tracer assays in the midbrain of 2-month-old zebrafish displaying examples of aneurysm severity in major vessels. 70 kDa Dextran–Fluorescein and 2000 kDa Dextran– Tetramethylrhodamine were co-injected to detect tracer extravasation to the brain parenchyma and tracer within the vasculature, respectively.
a', Confocal projections zoomed in on the area shown in **a** (dashed square). Aneurysm (arrowheads) phenotypes were qualitatively categorised based on severity; normal, mild and severe and these categories used in **Fig. 2**.

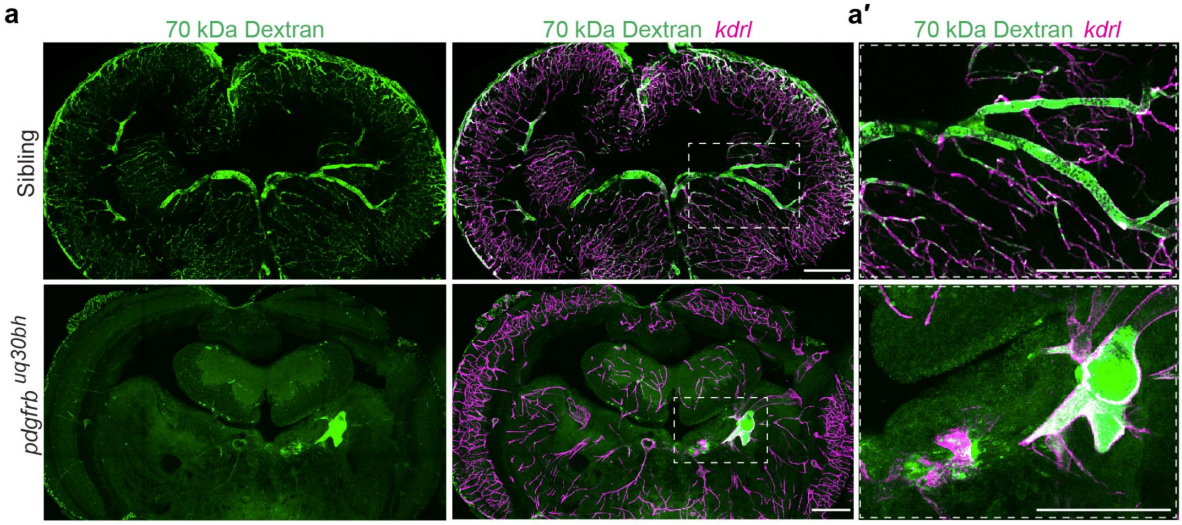

Extended Data Fig. 3

Adult *pdgfrb*^{uq30bh}mutant animals display leakage and tracer accumulation localised at major vessel aneurysms.

a, Fluorescent tracer leakage assays in 5-month-old sibling and *pdgfrb*^{uq30bh} animals. 70 kDa Dextran–Fluorescein (green) was retro-orbitally injected, and *Tg(kdrl:Hsa.HRAS-mCherry)*^{s843} was used to label the blood vessels (magenta). Scale bar: 250 µm.

a', Zoomed regions (dashed rectangles) from **a** highlighting the tracer accumulation outside the large calibre vessels with aneurysm. Scale bar: 250 µm.

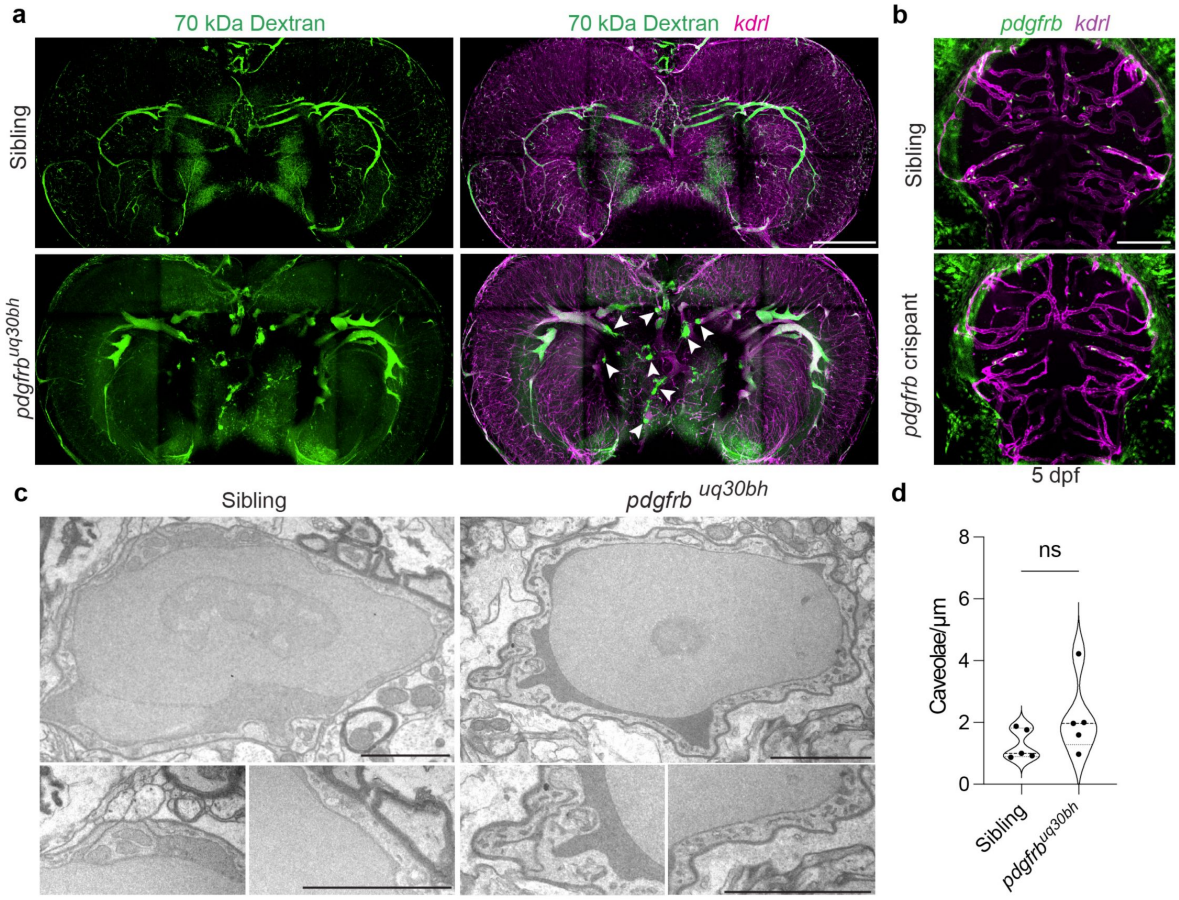

Extended Data Fig. 4

Adult *pdgfrb* mutant rupture hotspots at aneurysms and unchanged endothelial ultrastructure in capillaries.

a, Whole brain imaging showing midbrain vasculature (*Tg(kdrl:Hsa.HRAS-mCherry)*^{s843}) and 70 kDa Dextran–Fluorescein (green) in siblings and *pdgfrb*^{uq30bh} mutants at 5-months of age. Hotspot leakage sites are indicated by white arrowheads.
b, Confocal projections of pericytes (*TgBAC(pdgfrb:egfp)*^{ncv22}) and brain vasculature (*Tg(kdrl:Hsa.HRAS-mCherry)*^{s843}) in sibling and *pdgfrb* crispants at 5 dpf, showing loss of pericytes in the *pdgfrb* crispants (phenocopying null mutants).
c, Quantification of endothelial caveolae in capillaries of siblings and *pdgfrb*^{uq30bh} mutants. n=5 vessels per group, unpaired *t*-test ns= not significant.

References

1 Zhao Z., Nelson A. R., Betsholtz C., Zlokovic B. V 2015) **Establishment and Dysfunction of the Blood-Brain Barrier** *Cell* **163**:1064–1078 https://doi.org/10.1016/j.cell.2015.10.067

2 Armulik A., Genove G., Betsholtz C 2011) **Pericytes: developmental, physiological, and pathological perspectives, problems, and promises** *Dev Cell* **21**:193–215 https://doi.org/10.1016/j.devcel.2011.07.001

3 Leveen P., et al. 1994) **Mice deficient for PDGF B show renal, cardiovascular, and hematological abnormalities** *Genes Dev* **8**:1875–1887 https://doi.org/10.1101/gad.8.16.1875

4 Lindahl P., Johansson B. R., Leveen P., Betsholtz C 1997) **Pericyte loss and microaneurysm formation in PDGF-B-deficient mice** *Science* **277**:242–245 https://doi.org/10.1126/science.277.5323.242

5 Armulik A., et al. 2010) **Pericytes regulate the blood-brain barrier** *Nature* **468**:557–561 https://doi.org/10.1038/nature09522

6 Daneman R., Zhou L., Kebede A. A., Barres B. A 2010) **Pericytes are required for blood-brain barrier integrity during embryogenesis** *Nature* **468**:562–566 https://doi.org/10.1038/nature09513

7 Eilken H. M., et al. 2017) **Pericytes regulate VEGF-induced endothelial sprouting through VEGFR1** *Nat Commun* **8** https://doi.org/10.1038/s41467-017-01738-3

8 Simonavicius N., et al. 2012) **Pericytes promote selective vessel regression to regulate vascular patterning** *Blood* **120**:1516–1527 https://doi.org/10.1182/blood-2011-01-332338

9 Benjamin L. E., Hemo I., Keshet E 1998) **A plasticity window for blood vessel remodelling is defined by pericyte coverage of the preformed endothelial network and is regulated by PDGF-B and VEGF** *Development* **125**:1591–1598 https://doi.org/10.1242/dev.125.9.1591

10 Hellstrom M., Kalen M., Lindahl P., Abramsson A., Betsholtz C 1999) **Role of PDGF-B and PDGFR-beta in recruitment of vascular smooth muscle cells and pericytes during embryonic blood vessel formation in the mouse** *Development* **126**:3047–3055 https://doi.org/10.1242/dev.126.14.3047

11 Hirschi K. K., Rohovsky S. A., D'Amore P. A. PDGF 1998) **TGF-beta, and heterotypic cell-cell interactions mediate endothelial cell-induced recruitment of 10T1/2 cells and their differentiation to a smooth muscle fate** *J Cell Biol* **141**:805–814 https://doi.org/10.1083/jcb.141.3.805

12 Soriano P 1994) **Abnormal kidney development and hematological disorders in PDGF beta-receptor mutant mice** *Genes Dev* **8**:1888–1896 https://doi.org/10.1101/gad.8.16.1888

13 Ando K., et al. 2021) **Conserved and context-dependent roles for pdgfrb signaling during zebrafish vascular mural cell development** *Dev Biol* **479**:11–22 https://doi.org/10.1016/j.ydbio.2021.06.010

14 Mae M. A., et al. 2021) **Single-Cell Analysis of Blood-Brain Barrier Response to Pericyte Loss** *Circ Res* **128**:e46–e62 https://doi.org/10.1161/CIRCRESAHA.120.317473

15 Jeong J. Y., et al. 2008) **Functional and developmental analysis of the blood-brain barrier in zebrafish** *Brain Res Bull* **75**:619–628 https://doi.org/10.1016/j.brainresbull.2007.10.043

16 Xie J., Farage E., Sugimoto M., Anand-Apte B 2010) **A novel transgenic zebrafish model for blood-brain and blood-retinal barrier development** *BMC Dev Biol* **10** https://doi.org/10.1186/1471-213X-10-76

17 Quinonez-Silvero C., Hubner K., Herzog W 2020) **Development of the brain vasculature and the blood-brain barrier in zebrafish** *Dev Biol* **457**:181–190 https://doi.org/10.1016/j.ydbio.2019.03.005

18 Umans R. A., et al. 2017) **CNS angiogenesis and barriergenesis occur simultaneously** *Dev Biol* **425**:101–108 https://doi.org/10.1016/j.ydbio.2017.03.017

19 O'Brown N. M., Megason S. G., Gu C 2019) **Suppression of transcytosis regulates zebrafish blood-brain barrier function** *eLife* **8** https://doi.org/10.7554/eLife.47326

20 Ando K., et al. 2016) **Clarification of mural cell coverage of vascular endothelial cells by live imaging of zebrafish** *Development* **143**:1328–1339 https://doi.org/10.1242/dev.132654

21 Chen J., Poskanzer K. E., Freeman M. R., Monk K. R 2020) **Live-imaging of astrocyte morphogenesis and function in zebrafish neural circuits** *Nat Neurosci* **23**:1297–1306 https://doi.org/10.1038/s41593-020-0703-x

22 Ando K., et al. 2019) **Peri-arterial specification of vascular mural cells from naive mesenchyme requires Notch signaling** *Development* **146** https://doi.org/10.1242/dev.165589

23 Matsumoto K., et al. 2019) **Advanced CUBIC tissue clearing for whole-organ cell profiling** *Nat Protoc* **14**:3506–3537 https://doi.org/10.1038/s41596-019-0240-9

24 Pugach E. K., Li P., White R., Zon L 2009) **Retro-orbital injection in adult zebrafish** *J Vis Exp* https://doi.org/10.3791/1645

25 Sinha B., et al. 2011) **Cells respond to mechanical stress by rapid disassembly of caveolae** *Cell* **144**:402–413 https://doi.org/10.1016/j.cell.2010.12.031

26 Del Pozo M. A., Lolo F. N., Echarri A 2021) **Caveolae: Mechanosensing and mechanotransduction devices linking membrane trafficking to mechanoadaptation** *Curr Opin Cell Biol* **68**:113–123 https://doi.org/10.1016/j.ceb.2020.10.008

27 Rajan A. M., Ma R. C., Kocha K. M., Zhang D. J., Huang P 2020) **Dual function of perivascular fibroblasts in vascular stabilization in zebrafish** *PLoS Genet* **16**:e1008800 https://doi.org/10.1371/journal.pgen.1008800

28 Andreone B. J., et al. 2017) **Blood-Brain Barrier Permeability Is Regulated by Lipid Transport-Dependent Suppression of Caveolae-Mediated Transcytosis** *Neuron* **94**:581–594 https://doi.org/10.1016/j.neuron.2017.03.043

29 Boye K., et al. 2022) **Endothelial Unc5B controls blood-brain barrier integrity** *Nat Commun* **13** https://doi.org/10.1038/s41467-022-28785-9

30 Ayloo S., et al. 2022) **Pericyte-to-endothelial cell signaling via vitronectin-integrin regulates blood-CNS barrier** *Neuron* **110**:1641–1655 https://doi.org/10.1016/j.neuron.2022.02.017

31 Park D. Y., et al. 2017) **Plastic roles of pericytes in the blood-retinal barrier** *Nat Commun* **8**:15296 https://doi.org/10.1038/ncomms15296

1 Ando K., et al. 2016) **Clarification of mural cell coverage of vascular endothelial cells by live imaging of zebrafish** *Development* **143**:1328–1339 https://doi.org/10.1242/dev.132654

2 Chi N. C., et al. 2008) **Foxn4 directly regulates tbx2b expression and atrioventricular canal formation** *Genes Dev* **22**:734–739 https://doi.org/10.1101/gad.1629408

3 Jin S. W., Beis D., Mitchell T., Chen J. N., Stainier D. Y. 2005) **Cellular and molecular analyses of vascular tube and lumen formation in zebrafish** *Development* https://doi.org/10.1242/dev.02087

4 Traver D., et al. 2003) **Transplantation and in vivo imaging of multilineage engraftment in zebrafish bloodless mutants** *Nat Immunol* **4**:1238–1246 https://doi.org/10.1038/ni1007

5 Pugach E. K., Li P., White R., Zon L 2009) **Retro-orbital injection in adult zebrafish** *J Vis Exp* https://doi.org/10.3791/1645

6 Matsumoto K., et al. 2019) **Advanced CUBIC tissue clearing for whole-organ cell profiling** *Nat Protoc* **14**:3506–3537 https://doi.org/10.1038/s41596-019-0240-9

7 Davis A. E., Castranova D., Weinstein B. M. 2021) **Rapid Generation of Pigment Free, Immobile Zebrafish Embryos and Larvae in Any Genetic Background Using CRISPR-Cas9 dgRNPs** *Zebrafish* **18**:235–242 https://doi.org/10.1089/zeb.2021.0011

8 Lim Y. W., et al. 2017) **Caveolae Protect Notochord Cells against Catastrophic Mechanical Failure during Development** *Curr Biol* **27**:1968–1981 https://doi.org/10.1016/j.cub.2017.05.067

9 Isogai S., Horiguchi M., Weinstein B. M 2001) **The vascular anatomy of the developing zebrafish: an atlas of embryonic and early larval development** *Dev Biol* **230**:278–301 https://doi.org/10.1006/dbio.2000.9995

10 Schindelin J., et al. 2012) **Fiji: an open-source platform for biological-image analysis** *Nat Methods* https://doi.org/10.1038/nmeth.2019

Author information

Oguzhan F Baltaci

Organogenesis and Cancer Program, Peter MacCallum Cancer Centre, Melbourne, Australia, Sir Peter MacCallum Department of Oncology, University of Melbourne, Melbourne, Australia

Andrea Usseglio Gaudi

Organogenesis and Cancer Program, Peter MacCallum Cancer Centre, Melbourne, Australia, Sir Peter MacCallum Department of Oncology, University of Melbourne, Melbourne, Australia

Stefanie Dudczig
Organogenesis and Cancer Program, Peter MacCallum Cancer Centre, Melbourne, Australia, Sir Peter MacCallum Department of Oncology, University of Melbourne, Melbourne, Australia

Weili Wang
Institute for Molecular Bioscience, The University of Queensland, Brisbane, Australia

Maria Cristina Rondon-Galeano
Organogenesis and Cancer Program, Peter MacCallum Cancer Centre, Melbourne, Australia, Sir Peter MacCallum Department of Oncology, University of Melbourne, Melbourne, Australia

Ye-Wheen Lim
Institute for Molecular Bioscience, The University of Queensland, Brisbane, Australia

James Rae
Institute for Molecular Bioscience, The University of Queensland, Brisbane, Australia

Anne Lagendijk
Institute for Molecular Bioscience, The University of Queensland, Brisbane, Australia
ORCID iD: 0000-0003-1246-1608

Robert G Parton
Institute for Molecular Bioscience, The University of Queensland, Brisbane, Australia, Centre for Microscopy and Microanalysis, The University of Queensland, Brisbane, Australia
ORCID iD: 0000-0002-7494-5248

Alison Farley
Organogenesis and Cancer Program, Peter MacCallum Cancer Centre, Melbourne, Australia, Sir Peter MacCallum Department of Oncology, University of Melbourne, Melbourne, Australia, Walter and Eliza Hall Institute of Medical Research, Melbourne, Australia

Benjamin M Hogan
Organogenesis and Cancer Program, Peter MacCallum Cancer Centre, Melbourne, Australia, Sir Peter MacCallum Department of Oncology, University of Melbourne, Melbourne, Australia, Department of Anatomy and Physiology, University of Melbourne, Melbourne, Australia
ORCID iD: 0000-0002-0651-7065

For correspondence: ben.hogan@petermac.org

Editors

Reviewing Editor
Benoit Vanhollebeke
Université Libre de Bruxelles, Gosselies, Belgium

Senior Editor
Didier Stainier
Max Planck Institute for Heart and Lung Research, Bad Nauheim, Germany

Reviewer #1 (Public review):

Summary:

The study investigates the role of vascular mural cells, specifically pericytes and vascular smooth muscle cells (vSMCs), in maintaining blood-brain barrier (BBB) integrity and regulating vascular patterning. Analyzing zebrafish pdgfrb mutants that lack brain pericytes and vSMCs, they show that mural cell deficiency does not impair BBB establishment or maintenance during larval and early juvenile stages. However, mural cells seem to be crucial for preventing vascular aneurysms and hemorrhage in adulthood as focal leakage, basement membrane disruption, and increased caveolae formation are observed in adult zebrafish at aneurysm hotspots. The authors challenge the paradigm that mural cells are essential for BBB regulation in early development while highlighting their importance for long-term vascular stability.

Strengths:

Previous studies have established that the zebrafish BBB shares molecular and morphological homology with e.g. the mammalian BBB and therefore represents a suitable model. By examining mural cell roles across different life stages - from larval to adult zebrafish - the study provides an unprecedented comprehensive developmental analysis of brain vascular development and of how mural cells influence BBB integrity and vascular stability over time. The use of live imaging, whole-brain clearing, and electron microscopy offers high-resolution insights into cerebrovascular patterning, aneurysm development, and structural changes in endothelial cells and basement membranes. By analyzing "leakage hotspots" and their association with structural endothelial defects in adults the presented findings add novel insights into how mural cell loss may lead to vascular instability.

Weaknesses:

The study uses quantitative tracer assays with multiple molecular weight dyes to evaluate blood-brain barrier (BBB) permeability. The study normalizes the intensity of tracer signals (e.g., 10 kDa, 70 kDa dextrans) in the brain parenchyma to the vascular signal of a 2000 kDa dextran tracer (assumed to remain within vessels). Intensity normalization is used to control for variations in tracer injection efficiency or vascular density. This method doesn't directly assess the absolute amount of tracer present in the parenchyma, potentially underestimating leakage severity. As the lack of BBB impairment is a "negative" finding, more rigorous controls or other methods might be needed to corroborate it.

https://doi.org/10.7554/eLife.104061.1.sa2

Reviewer #2 (Public review):

Summary:

The authors generated a zebrafish mutant of the pdgfrb gene. The presented analyses and data confirm previous studies demonstrating that Pdgfrb signaling is necessary for mural cell development in zebrafish. In addition, the data support previously published studies in zebrafish showing that mural cell deficiency leads to hemorrhages later in life. The authors presented quantified data on vessel density and branching, assessed tracer extravasation, and investigated the vasculature of adult mice using electron microscopy.

Strengths:

The strength of this article is that it provides independent confirmation of the important role of Pdgfrb signaling for the development of mural cells in the zebrafish brain. In addition, it

confirms previous literature on zebrafish that provides evidence that, in the absence of pericytes/VSMC, hemorrhages appear (Wang et al, 2014, PMID: 24306108 and Ando et al 2021, PMID: 3431092). The study by Ando et al, 2021 did not report experiments assessing BBB leakage in pdgfrb mutants but in the review article by Ando et al (PMID: 34685412) it is stated that "indicating that endothelial cells can produce basic barrier integrity without pericytes in zebrafish".

Weaknesses:

(1) The authors should avoid using violin plots, which show distribution. Instead, they should replace all violin plots in the figures with graphs showing individual data points and standard deviation. For Figure 2f specifically, the standard deviation in the analyzed cohort should be shown.

(2) The authors have not shown the reduced PDGFRB protein or the effect of mutation on mRNA level in their zebrafish mutant.

(3) Statistical data analysis: Did the authors perform analyses to investigate whether the data has a normal distribution (e.g., Figures 1d, e)?

(4) Analysis of tracer extravasation. The use of 2000 kDa dextran intensity as an internal reference is problematic because the authors have not provided data demonstrating that the 2000 kDa dextran signal remains consistent across the entire vasculature. The authors have not provided data demonstrating that the 2000 kDa dextran signal in vessels exhibits acceptable variance across the vasculature to serve as a reliable internal reference. The variability of this signal within a single animal remains unknown. The presented data do not address this aspect.

Additionally, it's intriguing that the signal intensity in the parenchyma of the tested tracers presents a substantial range, varying by 20-30% in the analysed cohort (Figure 1g, Extended Figure 1e). Such large variability raises the question of its origin. Could it be a consequence of the normalization to 2000 kDa dextran intensity which differs between different fish? Or is it due to the differences in the parenchymal signal intensity while the baseline 2000 kDa intensity is stable? Or is the situation mixed?

An alternative and potentially more effective approach would be to cross the pdgfrb mutant line with a line where endothelial cells are genetically labeled to define vessels (e.g. the line kdrl used in acquiring data presented in Figure 2a). Non-injected controls could then be used as a baseline to assess tracer extravasation into the parenchyma.

How is the data presented in Figure 3e generated? How was the dextran intensity calculated? It looks like the authors have used the kdrl line to define vessels. Was the 2000 kDa still used as in previous figures? If not, please describe this in the Materials and Methods section.

(5) The authors state that both controls and mutants show extravasation of 1 kDa NHS-ester into the parenchyma. However, the presented images do not illustrate this; it is not obvious from these images (Extended Data Figure 1c). Additionally, the presented quantification data (Extended Data Figure 1e) do not show that, at 7 dpf, the vasculature is permeable to this tracer. Note that the range of signal intensity of the 1 kDa NHS-ester is similar to the 70 kDa dextran (Figure 1g and Extended Figure 1e). Would one expect an increase in the ratio in case of extravasation, considering that the 2000 kDa dextran has the same intensity in all experiments? Please explain.

(6) The study would be strengthened by a more detailed temporal analysis of the phenotype. When do the aneurysms appear? Is there an additional loss of VSMC?

(7) The authors intended to analyze the BBB at later stages (line 128), but there is not a significant time difference between 2 months (Figure 2) and 3 months (Figure 3) considering that zebrafish live on average 3 years. Therefore, the selection of only two time-points, 2 and 3 months, to analyze BBB changes does not provide a comprehensive overview of temporal changes throughout the zebrafish's lifespan. How long do the pdgfb mutants live?

(8) Why is there a difference in tracer permeability between 2 and 3 months (Figures 2 and 3)? Are hemorrhages not detected in 2-month-old zebrafish?

(9) Figure 3: The capillary bed should be presented in magnified images as it is not clearly visible. Figure 3e shows that in the pdgfb mutant the dextran intensity is higher also in regions 6-10. How do the authors explain this?

(10) In general, the manuscript would benefit from a more detailed description of the performed experiments. How long did the tracer circulate in the experiments presented in Figures 2, 3, and 4?

(11) How do the authors explain the poor signal of the 70 kDa dextran from the vasculature of 5-month-old zebrafish presented in Extended Data Figure 3?

(12) The study would benefit from a clear separation of the phenotypes caused by the loss of VSMC. The title eludes that also capillaries present hemorrhages which is not the case. How do vascular mural cells differ from mural cells? Are there any other mural cells?

(13) I have a few comments about how the authors have interpreted the literature and why, in my opinion, they should revise their strong statements (e.g., the last sentence in the abstract).

Scientists have their own insights and interpretations of data. However, when citing published data, it should be clearly indicated whether the statement is a direct quote from the original publication or an interpretation. In the current manuscript, the authors have not correctly cited the data presented in the two published papers (references 5 and 6). These papers do not propose a model where pericytes suppress "adsorptive transcytosis" (lines 73-76). While increased transcytosis is observed in pericyte-deficient mice, the specific type of vesicular transport that is increased or induced remains unknown.

Similarly, lines 151-152 refer to references 5 and 6 and use the term "adsorptive transcytosis," but the authors of both papers did not use this term. Attributing this term to the original authors is inaccurate. Additionally, lines 152-153 do not accurately represent the findings of references 5 and 6. These papers do not state that there is an induction of "caveolae" in endothelial cells in pericyte-deficient mice. In the absence of pericytes, many vesicles can be observed in endothelial cells, but these vesicles are relatively large. It is more likely that there is some form of uncontrolled transcytosis, perhaps micropinocytosis. Please refer to the original papers accurately.

Also, the authors have missed the fact that in mice, the extent of pericyte loss correlates with the extent of BBB leakage. To a certain extent, the remaining pericytes, can compensate for the loss by making longer processes and so ensure the full longitudinal coverage of the endothelium. This was shown in the initial work of Armulik et al (reference 5) and later in other studies.

The bold assertion on lines 183 -187 that a lack of specific BBB phenotype in pdgfrb zebrafish mutant invalidates mouse model findings is unfounded. Despite the notion that zebrafish endothelium possesses a BBB, I present a few examples highlighting the differences in brain vascular development and why the authors' expectation of a straightforward extrapolation of mouse BBB phenotypes to zebrafish is untenable.

In mice Pdgfrb knockout is lethal, but in zebrafish, this is not the case. In marked contrast to mice, however, zebrafish pdgfrb null mutants reach adulthood despite extensive cerebral vascular anomalies and hemorrhage. Following the authors' argumentation about the unlikely divergence of zebrafish and mice evolution, does it mean that the described mouse phenotype warrants a revisit and that the Pdgfrb knockout in mice perhaps is not lethal? Another example where the role of a gene product is not one-to-one, which relates to pericyte development, is Notch3. Notch3-null mice do not show significant changes in pericyte numbers or distribution, suggesting a less prominent role in pericyte development compared to zebrafish.

Although many aspects of development are conserved between species, there are significant differences during brain vascular development between zebrafish and mice. These differences could reveal why the BBB is not impaired in zebrafish pdgfrb mutants. There is a difference in the temporal aspect when various cellular players emerge. The timing of microglia colonization in the brain differs. In mice, microglia colonization starts before the first vessel sprouts enter the brain, while in zebrafish, microglia enter after. Additionally, microglia in zebrafish and mice have a different ontogeny. In mice, astrocytes specialize postnatally and form astrocyte endfeet postnatally. In zebrafish, radial glia/astrocytes form at 48 hpf, and as early as 3 dpf, gfap+ cells have a close relationship with blood vessels. Thus, these radial glia/astrocyte-like cells could play an important role in BBB induction in zebrafish. It's worth noting that in Drosophila, the blood-brain barrier is located in glial cells. While speculative, these cells might still play a role in zebrafish, while the role of pericytes does not seem to be crucial. Pericytes enter the brain and contact with developing vasculature (endothelium) relatively late in zebrafish (60 hpf). In mice, the situation is different, as there is no such lag between endothelium and pericyte entry into the brain. I suggest that the authors approach the observed data with curiosity and ask: Why are these differences present? Are all aspects of the BBB induced by neural tissue in zebrafish? What is the contribution of microglia and astrocytes?"

Another interesting aspect to consider is the endothelial-pericyte ratio and longitudinal coverage of pericytes in the zebrafish brain, and how this relates to what is observed in mice. How similar is the zebrafish vasculature to the mouse vasculature when it comes to the average length of pericytes in the zebrafish brain? Does the longitudinal coverage of pericytes in the zebrafish brain reach nearly 100%, as it does in mice?

Based on the preceding arguments, it is recommended that the authors present a balanced discussion that provides insightful discussion and situates their work within a broader framework.

https://doi.org/10.7554/eLife.104061.1.sa1

Reviewer #3 (Public review):

This manuscript examines the role of pdgfrb-positive pericytes in the establishment and maintenance of the blood-brain barrier (BBB) in the zebrafish. Previous studies in PDGFB- or PDGFRB-deficient mice have suggested that loss of pericytes results in disruption of the BBB. The authors show that zebrafish pdgfrb mutant larvae have an intact BBB and that pdgfrb mutant adult fish show large vessel defects and hemorrhage but do not exhibit substantial leakage from brain capillaries, suggesting loss of pericytes is not sufficient to "open" the BBB. The authors use beautiful and compelling images and rigorous quantification to back up most of their conclusions. The imaging of the adult brain is particularly nice. The authors rigorously document the lack of BBB leakage in pdgfrbuq30bh mutant larvae and large vessel phenotypes (eg, enlargement and rupture) in pdgfrbuq30bh mutant adults. A few points

would help the authors to further strengthen their findings contradicting the current dogma from rodent models.

Major point:

The authors document pericyte loss using a single TgBAC(pdgfrb:egfp)ncv22 transgenic line driven by the promoter of the same gene mutated in their pdgfrbuq30bh mutants. Given their findings on the consequences of pericyte loss directly contradict current dogma from rodent studies, it would be useful to further validate the absence of brain pericytes in these mutants using one of several other transgenic lines marking pericytes currently available in the zebrafish. This could be done using pdgfrb crispants, which the authors show nicely phenocopy the germline mutants, at least in larvae. This would help nail down the absence of any currently identifiable pericyte population or sub-population in the loss of pdgfrb animals and substantially strengthen the authors' conclusions.

Other issues:

The authors should provide more information about the pdgfrbuq30bh mutant and how it was generated (including a diagram in a supplemental figure would be useful).

It would be helpful to show some data on whether mutants show morphological phenotypes or developmental delay at 7 and 14 dpf, to provide some context to better assess the reduced branching and vessel length vascular phenotypes (see Figures 1c-e).

If available, it would be helpful to have a positive control for the tracer leakage experiments - a genetic manipulation that does cause disruption of the BBB and leakage at 2 hours post-tracer injection (see Figures 1f and g).

Quantification of the findings in Figure 4c,d would be useful, as would the use of germline fish for these experiments if these are now available. If this is not possible, it would be helpful to document that the crispants used in these experiments lack pdgfrb:egfp pericytes at adult stages (this is only shown for 5 dpf larvae, in Extended Data Figure 4b).

Adult mutants clearly show less dye leakage in the more superficial capillary regions than WT siblings, but dextran intensity is a bit higher, although this could well be diffusion from more central brain regions where overt hemorrhage is occurring. Along similar lines though, the authors' TEM data in Extended Data Figure 4d hints that there may be more caveolae in mutant brain capillaries, although the N number was lower here than for the measurements from TEM of larger central vessels (Figure 4g). It would be useful to carry out additional measurements to increase the N number in Figure 4d to see whether the difference between wild-type sibling and mutant capillary caveolae numbers remains as not significant.

It might be helpful to include some orienting labels and/or additional descriptions in the figure legends to help readers who are not used to looking at zebrafish brain vessels have an easier time figuring out what they are looking at and where it is in the brain.

https://doi.org/10.7554/eLife.104061.1.sa0

Author response:

We thank all the reviewers for their detailed comments. In response, we will address the comments with further analysis, experiments and an expanded discussion.

In terms of each specific reviewer's comments:

Reviewer 1 was positive overall but had several suggestions and requested further rigorously controls. These are highly constructive technical concerns and will be addressed through

additional experimentation and methods for quantification.

Reviewer 2 summarised the strengths of the study as being largely confirmatory. They have perhaps not fully appreciated that this is the first published functional assessment of cerebral vascular permeability in a pericyte deficient zebrafish model.

The reviewer has made a number of very helpful suggestions to improve technical aspects of the analysis. Many align with the suggestions of Reviewer 1. Additional experiments that include more rigorous controls and further methods to quantify vessel permeability will address these concerns in revision.

We also note that the reviewer calls for a more nuanced and careful discussion section. We take the reviewers point and do appreciate their concerns. We were limited by wordcount in the initial submission in short report format, but in response will expand and provide a more thorough discussion.

Reviewer 3 was positive overall but has suggested additional controls and experiments to further strengthen the findings and support our conclusions. Some align with the suggestions of Reviewers 1 and 2. We agree and aim to address them through additional work in revision.

https://doi.org/10.7554/eLife.104061.1.sa4